

S.A. Fayans

I.V. Kurchatov Institute for Atomic Energy, Moscow

N.I. Pyatov

Joint Institute for Nuclear Research, Dubna

### 1. Introduction

In the present work the theory of finite Fermi-systems is applied to description of the multipole (S=0) and spin-multipole (S=1) charge-exchange nuclear excitations. The experimental data on the isobaric analog states (IAS) and Gamow-Teller resonances (GTR) recently obtained from the (p,n) studies are used to specify some characteristics of the charge-exchange effective interactions which are then employed to predict properties of the L=1,2,3 resonances.

The calculations have shown that to reproduce the observed energy of IAS and its escape width, one should introduce the strong density dependence in the isovector interaction. Such a density dependence affects noticeably the energies of other multipole resonances.

The influence of the one-pion-exchange potential on the S=1 resonances is studied. The value of the Landau-Migdal parameter  $g'$  is deduced by comparing the calculated energies of the GTR with the experimental ones. The dependence of the strength functions on the momentum transfer is also studied. Our calculations have shown that the S=0 and S=1 resonances with the same spin and parity possess quite different properties.

The microscopic calculations were carried out for such isobaric pairs as  $^{56}\text{Fe}-^{56}\text{Co}$ ,  $^{90}\text{Zr}-^{90}\text{Nb}$  and  $^{208}\text{Pb}-^{208}\text{Bi}$  but in this short report we discuss mainly the results obtained for the latter case.

### 2. Effective interactions

The isospin-dependent interactions used in this paper were chosen in the form

$$\mathcal{F} = (1/2) (\mathcal{F}^- + G^- + G_\pi^-) \vec{\tau}_1 \cdot \vec{\tau}_2, \quad (1)$$

where

$$\mathcal{F}^- = 2C_0 [a'_\delta \delta(\vec{r}_1 - \vec{r}_2) + a'_v v(\vec{r}_1 - \vec{r}_2) - (b/2\rho_0)\rho^+ (\frac{\vec{r}_1 + \vec{r}_2}{2}) \delta(\vec{r}_1 - \vec{r}_2)],$$

$$G^- = 2C_0 g' \delta(\vec{r}_1 - \vec{r}_2) \vec{\sigma}_1 \cdot \vec{\sigma}_2,$$

$$G_\pi^- = 2C_0 g_\pi (1 - 2\zeta)^2 \frac{(\vec{\sigma}_1 \cdot \vec{q})(\vec{\sigma}_2 \cdot \vec{q})}{m_\pi^2 + q^2 + P_\Delta(q^2)}.$$

One can see that the isovector amplitude  $\mathcal{F}^-$  contains both the zero and finite range components and the term with the linear density dependence ( $\rho^+ = \rho_n + \rho_p$ ), the latter arising from the consistency condition between the irreducible amplitudes of two- and three-particle interactions<sup>1)</sup>. The function  $v$  is taken in the Yukawa form with the range  $r_0 = 0.8$  fm and is normalized as  $\int v(\vec{r}) d\vec{r} = 1$ .

The spin-isospin repulsive interaction  $G^-$  has the familiar Landau-Migdal form. It is generalized by including the direct one-pion-exchange amplitude  $G_\pi^-$  which contains both the effect of renormalization of the pion-nucleon interaction in nuclear matter and the contribution of virtual isobar-hole

excitations. The latter is effectively taken into account through the polarization operator  $P_\Delta = -0.9q^2 / (1 + 0.23q^2/m_\pi^2)$  (see, e.g. ref.<sup>2)</sup>).

The following parameters were fixed in calculations:  $\zeta = 0.05$ ,  $g_\pi = -1.15$ ,  $C_0 = 300$  MeV fm<sup>3</sup> and  $\rho_0 = 0.172$  fm<sup>-3</sup>.

The isotopic invariance of nuclear interactions gives rise to the consistency condition<sup>1)</sup> between  $\mathcal{F}^-$ , the isovector density  $\rho^- = \rho_n - \rho_p$  and the isovector potential  $U^-$ :

$$U^-(\vec{r}) = \int \mathcal{F}^-(\vec{r}, \vec{r}') \rho^-(\vec{r}') d\vec{r}'. \quad (2)$$

For a given  $U^-(\vec{r})$  this condition leads to the relation between strength parameters  $a'_\delta$ ,  $a'_v$  and  $b$ , which can be written in the form of an integral equation for the potential symmetry energy:

$$\int U^-(\vec{r}) \rho^-(\vec{r}) d\vec{r} = \int \rho^-(\vec{r}) \mathcal{F}^-(\vec{r}, \vec{r}') \rho^-(\vec{r}') d\vec{r} d\vec{r}' = 2\beta_{\text{sym}} (N-Z)^2 / A. \quad (3)$$

Note that the amplitudes  $G^-$  and  $G_\pi^-$  make no contribution to the self-consistent field, hence we have no consistency conditions for them.

### 3. Effective fields and strength functions

The charge-exchange (p,n<sup>-1</sup>) and (n,p<sup>-1</sup>) excitations are described by means of the effective fields  $V$  which appear in the nucleus upon the application of the external field  $V_0$ . The integral equation for  $V$  can be written<sup>3)</sup> in a symbolic form

$$V = e_q V^0 + \mathcal{F}AV, \quad (4)$$

where  $e_q$  is the local quasiparticle charge with respect to the field  $V_0$  and  $A$  the particle-hole propagator.

The external fields were taken as

$$V_L^0(r, q) = [(2L+1)!!/q^L] j_L(qr) Y_L \tau_\pm,$$

$$V_{LJ}^0(r, q, \sigma) = [(2L+1)!!/q^L] j_L(qr) [\sigma \times Y_L]^J \tau_\pm, \quad (5)$$

where  $j_L$  is the spherical Bessel function and  $q$  the momentum transfer. The former fields generate familiar S=0 multipole excitations, while the latter give rise to the S=1 spin-multipole ones with  $J=L, L\pm 1$ . In the limit  $q \rightarrow 0$  expressions (5) become the standard operators involved in allowed beta decays. In a general case, using eq. (5) one can study the form factors of resonance states as well as the redistribution of the transition strength over the excitation spectrum with changing  $q$ .

The excitation spectrum in the field  $V$  is characterized by the strength function<sup>3)</sup>

$$S(\omega, q) = -\frac{1}{\pi} \text{Im}(e_q V^0 A V), \quad (6)$$

where  $\omega$  is the excitation energy. The particle-hole propagators  $A$  are evaluated and eq. (4) for the effective field  $V$  is solved in the coordinate space which makes it possible to accurately allow for the one-particle continuum in our calculations. Thus we work here using the complete one-particle basis.

#### 4. Results and discussion

Given below are the numerical results for the isobaric pair  $^{208}\text{Pb}$ - $^{208}\text{Bi}$ . The one-particle basis was generated by the Woods-Saxon potential ( $r = n, p$ ):

$$U_r = -V_0^r \cdot f_r(r) - V_{\ell_s}^r \cdot (r_0^r)^2 \frac{1}{r} \frac{df_r}{dr} (\vec{\ell} \cdot \vec{s}),$$

$$f_r(r) = \left(1 + \exp \frac{r - R_r}{a}\right)^{-1}, \quad R_r = r_0^r A^{1/3}. \quad (7)$$

The Coulomb potential has a standard form corresponding to the uniformly charged sphere of the radius  $1.2A^{1/3}$  fm. The following values of the parameters are used:

$$V_0^n = 47 \text{ MeV}, \quad V_{\ell_s}^n = 21.1 \text{ MeV}, \quad r_0^n = 1.22 \text{ fm},$$

$$V_0^p = 60.2 \text{ MeV}, \quad V_{\ell_s}^p = 27.5 \text{ MeV}, \quad r_0^p = 1.26 \text{ fm},$$

$$a = 0.65 \text{ fm}. \quad (8)$$

Such a parametrization reproduces the experimental values for the rms charge radius  $\langle r_c^2 \rangle^{1/2} = 5.5$  fm and the neutron-proton rms difference  $\Delta r_{np} = 0.1$  fm. To reproduce the observed one-particle spectra near  $^{208}\text{Pb}$  the well depth  $V_0^r$  were varied within  $\approx 1$  MeV for each  $\ell j$ . Then the obtained one-particle basis was used in calculations for all the modes discussed below.

According to the consistency condition the isovector potential  $U_{WS}^- = U_n - U_p$  introduced through eq. (7) should coincide with the potential  $U^-$  given by eq. (2). We have tried to satisfy this condition using the following procedure. Equation (3) in which the quantities  $U^-$  and  $\rho^-$  are replaced by those corresponding to the Woods-Saxon potential (7) was used to determine the value of  $a_\delta'$ , the other parameters ( $a_r'$  and  $b$ ) being varied so as to achieve the best consistency between  $U^-$  (eq. (2)) and  $U_{WS}^-$  (especially in the surface region) and to obtain the experimental value 18.85 MeV for the IAS energy (Coulomb shift energy). The potentials  $U^-$  and  $U_{WS}^-$  prove to be close to each other in the surface region provided there is a strong density dependence in  $\mathcal{F}^-$  (see fig. 1). It should be noticed that the IAS energy increases from 16.3 to 18.85 MeV with the increase of  $b$  from 0 to 3.94. The variation of the strength of the finite range interaction  $a_r'$  does not affect

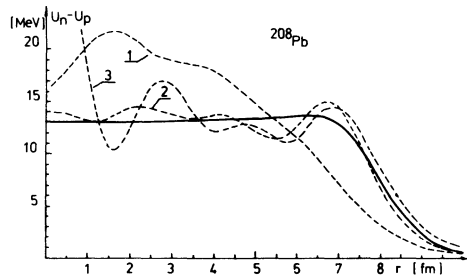


Fig. 1. The Woods-Saxon isovector potential  $U_{WS}^-$  (solid line) and self-consistent potentials  $U^-$  (dashed lines) calculated from eq. (2) with the parameters: 1)  $a_\delta' = 0.16$ ,  $a_r' = 0.8$ ,  $b = 0$ ; 2)  $a_\delta' = 1.72$ ,  $a_r' = 0.8$ ,  $b = 3.94$ ; 3)  $a_\delta' = 0$ ,  $a_r' = 2.66$ ,  $b = 4$ . In all the cases the calculated value of  $\beta_{\text{sym}}$  is equal to 29.5 MeV.

noticeably the IAS energy, but it plays an important part in smoothing down the volume oscillations of  $U^-$  and in changing its slope at the surface. For this reason we have used both the zero and finite range amplitudes in  $\mathcal{F}^-$  (compare curves 2 and 3 in fig. 1, both corresponding to the same IAS energy 18.85 MeV). Thus the following best-fit set of the parameters was obtained:

$$a_\delta' = 1.72, \quad a_r' = 0.8, \quad b = 3.94. \quad (9)$$

We would like to emphasize that the neutron skin thickness plays an important role in the fitting procedure. Indeed, if we use the Woods-Saxon potential with  $r_0^n = r_0^p = 1.24$  fm which yields  $\langle r_c^2 \rangle^{1/2} = 5.4$  fm and  $\Delta r_{np} = 0.23$  fm, then for any variations of the force parameters in  $\mathcal{F}^-$  satisfying eq. (3) the IAS appears at least 1 MeV below the observed one.

In terms of the force parameter  $f^- = 2f^r$  of the theory of finite Fermi systems<sup>3)</sup> the set (9) corresponds to the change of  $f^-$  from  $f_{in} \approx 1$  inside the nucleus to  $f_{ex}^- \approx 5$  outside of it. While such a sharp interpolation is needed to achieve an agreement between theory and experiment, it does not seem quite realistic. To elucidate this problem the fully self-consistent calculations are in progress now and the results will be published elsewhere. Anyhow it is already apparent that the density dependence of the  $\mathcal{F}^-$  interaction is of a crucial importance for the self-consistent description of the IAS and other  $S = 0$  multipole resonances. In order to demonstrate the effects expected due to the interpolation in the  $f^-$ -channel, we present below the results for the set (9) and for another one which satisfies relation (3) at  $b = 0$ , i.e. without any interpolation.

As to the spin-isospin interaction, the Landau-Migdal parameter  $g'$  was deduced by comparing the calculated energy of the GTR with the experimental one ( $\approx 19.2$  MeV with respect to the ground state of  $^{208}\text{Pb}$ ). In the case of  $g_\pi = 0$ , we have found  $g' = 0.95$ , while the inclusion of the one-pion exchange ( $g_\pi = -1.15$ ) increases  $g'$  to 1.1.

Shown in fig. 2 are the strength functions for the IAS and GTR calculated with the parameters (9) and  $g' = 1.1$ ,  $g_\pi = -1.15$ , respectively. Due to the influence of the one-particle continuum which is properly included in our calculations the resonance states above the neutron (proton) threshold in the daughter nucleus with  $T_Z = T_0 - 1$  ( $T_Z = T_0 + 1$ ) acquire the escape width  $\Gamma_{\text{esc}}$ . The estimates of  $\Gamma_{\text{esc}}$  are given in the figure. In the case of IAS, the value of  $\Gamma_{\text{esc}}$  is close to the total experimental width ( $\approx 230$  keV)<sup>5)</sup>;

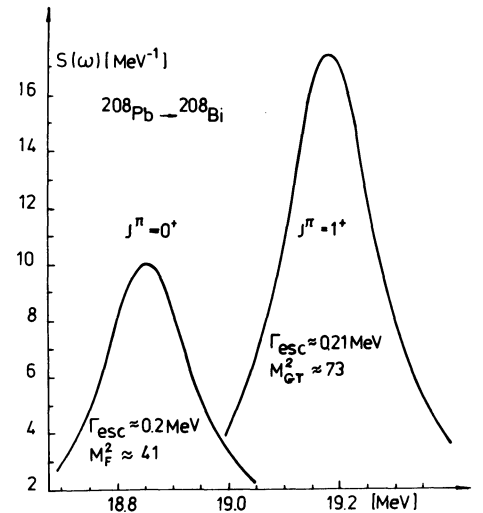


Fig. 2. Strength functions for the IAS and GTR in  $^{208}\text{Bi}$ . The energy is given with respect to the ground state of  $^{208}\text{Pb}$ .

in the case of GTR, the calculated  $\Gamma_{\text{esc}}$  is much smaller than the experimental width observed in (p,n)-reaction ( $\approx 4.1$  MeV)<sup>4</sup>). Such a difference is associated with the difference of the isotopic spin in these resonances. The beta-decay matrix elements shown in fig. 2 are also estimated on the basis of the strength functions obtained:

$$M^2 = 4\pi \int S(\omega, q=0) d\omega \approx 2\pi^2 \Gamma_{\text{esc}} S_{\text{max}}, \quad (10)$$

where  $S_{\text{max}}$  is the maximum value of  $S$ . The value of  $M_{\text{GT}}^2 \approx 73$  means that approximately 55% of the sum rule  $3(N-Z)$  for GT beta-decay is located in the GTR. This is 1.5 times greater than  $M_{\text{GT}}^2$  deduced from the (p,n) study<sup>4</sup>). To achieve an agreement with the experimental data, it is sufficient to introduce the local charge  $e_q[\sigma\tau] \approx (1-2\zeta_s) \approx 0.8$  for the axial-vector field in accordance with the traditional estimate  $\zeta_s < 0.1$ <sup>3</sup>). But our calculations for GTR in  $^{90}\text{Nb}$  yield  $M_{\text{GT}}^2 \approx 22$  which is about 3 times as large as the experimental result<sup>6</sup>). Such a big difference cannot be removed by introducing the local charge alone. The pairing correlations in the ground state of  $^{90}\text{Zr}$  do not essentially improve the situation since these correlations reduce  $M_{\text{GT}}^2$  by approximately 15% only. Thus the problem of the GT strength quenching in medium and heavy nuclei remains open.

To simplify the numerical calculations for greater energy intervals, we introduced the shift  $\gamma_D$  of the poles of the one-particle Green functions into the complex plane (i.e., the damping of quasiparticles). As a result, all the states acquire the artificial width  $\Gamma_D = 4\gamma_D$  in addition to the escape width. This procedure, of course, does not affect the sum rule. All the results discussed below (figs. 3-6) are obtained with  $\Gamma_D = 1$  MeV.

In fig. 3 there are shown the strength functions for the  $J^\pi = 1^+(L=0)$  excitations in  $^{208}\text{Bi}$  calculated for several sets of parameters  $g'$  and  $g_\pi$  as well as for various momentum transfers. It is seen that the effective interactions change essentially the distribution of the transition probability and give rise to the GTR. The inclusion of the one-pion exchange does not change qualitatively the behaviour of the strength function at  $q=0$ . The arrowed numbers in the upper part of fig. 3 show the relative contribution of the  $1^+$  excitations to the sum rule up to the corresponding energy (for  $e_q[\sigma\tau]=1$ ), approximately 90 per cent of the sum rule being exhausted below 40 MeV. One can see from the lower part of fig. 3 that the shape of the strength function changes essentially with the increase of  $q$ . For  $q=1 \text{ fm}^{-1}$  we observe the relative increase of  $S(\omega)$  in the low-energy region, the peak in the GTR region almost disappearing and the new broad peak appearing in the vicinity of 25 MeV. We should like to emphasize that the one-pion exchange is largely responsible for the relative enhancement of  $S(\omega)$  at small energies though the value of  $g' = 1.1$  used in the calculations is noticeably greater than the estimated critical value of  $g'_{\text{cr}} \approx 0.6$  which corresponds to the instability of the pion-like modes with positive parity for the nuclei considered.

Figs. 4-6 display the strength functions  $S(\omega, q=0)$  for the multiplets of excitations with  $L=1, 2, 3$ . Horizontal bars in figs. 4 and 5 indicate the locations and widths of the  $L=1$  and  $L=2$  resonances observed in the (p,n) experiment<sup>4,7</sup>). The one-pion exchange potential contributes to  $S(\omega)$  only in the  $J=L \pm 1$  cases (parts a and b in these figures), while in the  $J=L$  cases  $S(\omega)$  depends on both the  $G^-$  and  $F^-$  amplitudes, the spin-flip ( $S=1$ ) resonances (part c) being mainly sensitive to the variation of the parameter  $g'$ , and the  $S=0$  resonances (parts d), to the variation of the force parameters in  $F^-$ . It can be seen that the interactions shift the unperturbed distributions with  $L=1$

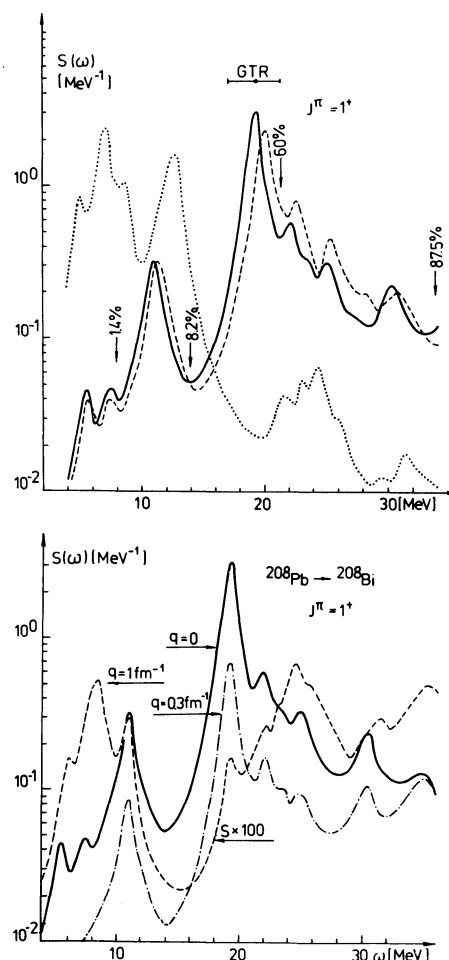


Fig. 3. Strength functions for the  $1^+$ ,  $L=0$  excitations in  $^{208}\text{Bi}$ . Upper part:  $S(\omega, q=0)$  at  $g' = g_\pi = 0$  (dotted line), at  $g' = 1.1, g_\pi = 0$  (dashed line) and at  $g' = 1.1, g_\pi = -1.15$  (solid line). Lower part:  $S(\omega, q)$  at  $g' = 1.1, g_\pi = -1.15$  for various  $q$ . The location and the width of the GTR<sup>4</sup>) are shown with the horizontal bar.

and  $L=2$  (shown by dotted lines) in the right direction and make the resonance structure in  $S(\omega)$  much more pronounced. For the  $L=3$  excitations, the distributions come out fragmented.

The inclusion of the density dependence in  $F^-$  noticeably pushes the  $S=0$  resonance up. In the dipole case for example, the maximum of the corresponding distribution shifts through almost 4 MeV as  $b$  increases from 0 to  $\approx 4$  which should be compared with the 2.5 MeV shift in the case of IAS.

The influence of the one-pion exchange on  $S(\omega)$  is also noticeable. One can note that its effect on the resonance energies cannot be simulated by a simple renormalization of  $g'$  because this renormalization greatly depends on  $L$ . Indeed, when  $g_\pi \rightarrow 0$  we should decrease  $g'$  from 1.1 to 0.65 in order to keep the  $0^-$  resonance at 28 MeV. If the same procedure is applied to the GTR the value of  $g'$  should be decreased from 1.1 to 0.95 only, as was mentioned above. In the case of the  $L=2$  spin-quadrupole resonance with  $S=1$  (fig. 5) the corresponding decrease of  $g'$  is even more pronounced.

By comparing our results with the experimental data<sup>4,7</sup>) the conclusion can be drawn that in the regions of the observed  $L=1, 2$  resonances one should expect the contribution from all the spin-multiplet modes.

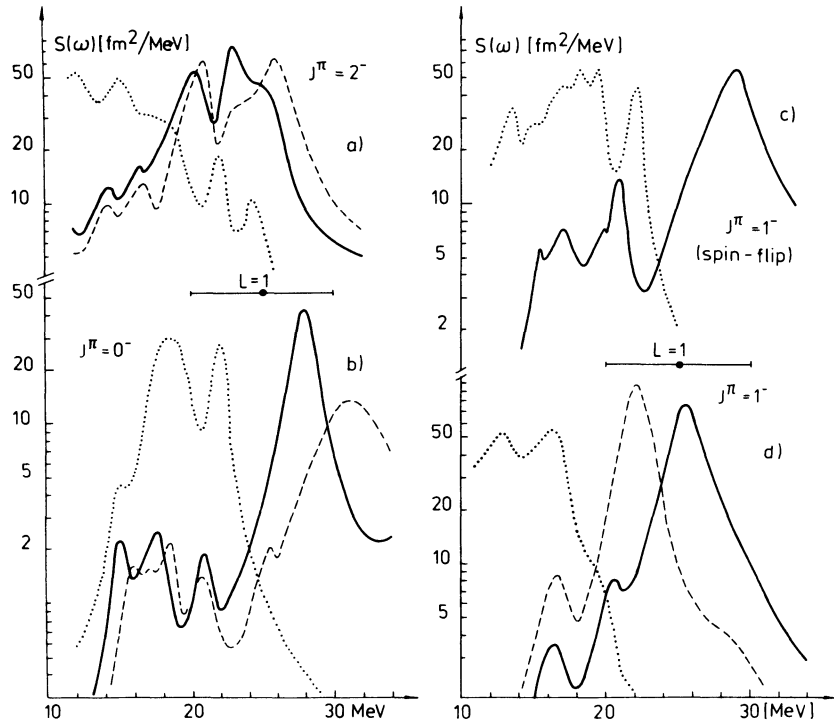


Fig. 4. Strength functions  $S(\omega, q=0)$  for the  $L=1$ ,  $S=0,1$ -excitations in  $^{208}\text{Bi}$ . Dotted lines: unperturbed  $S(\omega, q=0)$  when the effective interactions are switched off; dashed (solid) lines in parts a) and b): calculations at  $g'=1.1$ ,  $g_\pi=0$  ( $g'=1.1$ ,  $g_\pi = -1.15$ ); solid lines in parts c) and d): calculations with the force parameters of eq. (9) and with  $g'=1.1$ ; dashed line in part d):  $S(\omega, q=0)$  at  $b=0$  (this case corresponds to the curve 1 in fig. 1); horizontal bars: the location and the width of the  $L=1$  resonance<sup>4,7</sup>).

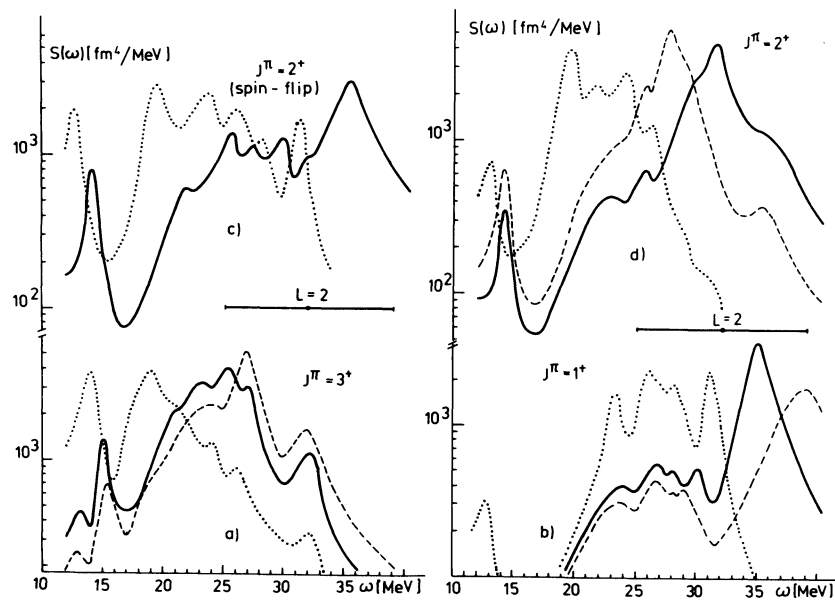


Fig. 5. As in fig. 4 but for the  $L=2$  excitations.

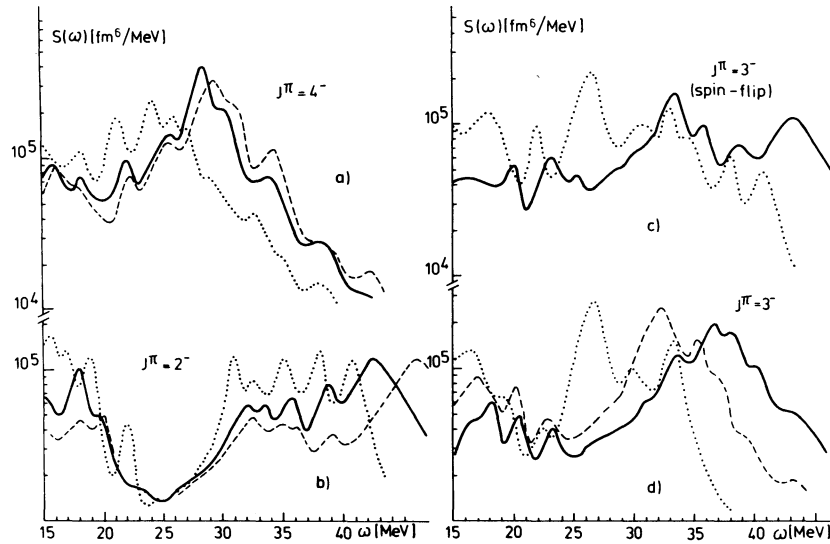


Fig. 6. As in fig. 4 but for the  $L=3$  excitations and dashed lines in parts a) and b) corresponding to  $g'=0.95$  and  $g_{\pi}=0$ .

#### Acknowledgements

We wish to thank V.V.Palichik for assistance with the calculations.

#### References

1. V.A. Khodel. *Yad.Fiz.* **19**, 792 (1974).  
S.A.Fayans and V.A.Khodel. *JETP Lett.* **17**, 444 (1973).  
E.E.Saperstein, S.A.Fayans and V.A.Khodel. *Particles and Nuclei*, **9**, 222 (1978).
2. A.B.Migdal. *Rev.Mod.Phys.*, **50**, 107 (1978).  
S.A.Fayans, E.E.Saperstein and S.V.Tolokonnikov. *Nucl.Phys.*, **A326**, 463 (1979).
3. A.B.Migdal. *Theory of finite Fermi systems and applications to atomic nuclei* (Interscience, New York, 1967).
4. D.J.Horen et al. *Phys.Lett.*, **95B**, 27 (1980).
5. E.C. Booth and B.S.Madsen. *Nucl.Phys.*, **A206**, 293 (1973).
6. D.E.Bainum et al. *Phys.Rev.Lett.*, **44**, 1751 (1980).
7. C.Gaarde et al. *Excitation of giant spin-isospin multipole vibrations*. Preprint, 1981.